Electron scattering cross sections from HCN over a broad energy range (0.1–10000 eV): Influence of the permanent dipole moment on the scattering process

A. G. Sanz, M. C. Fuss, F. Blanco, F. Sebastianelli, F. A. Gianturco et al.

Citation: J. Chem. Phys. **137**, 124103 (2012); doi: 10.1063/1.4754661
View online: http://dx.doi.org/10.1063/1.4754661
View Table of Contents: http://jcp.aip.org/resource/1/JCPSA6/v137/i12
Published by the American Institute of Physics.

Electron scattering cross sections from HCN over a broad energy range (0.1–10 000 eV): Influence of the permanent dipole moment on the scattering process

A. G. Sanz,[1] M. C. Fuss,[1] F. Blanco,[2,a)] F. Sebastianelli,[3] F. A. Gianturco,[3] and G. García[1,4]

[1]*Instituto de Física Fundamental, Consejo Superior de Investigaciones Científicas, Serrano 113-bis, 28006 Madrid, Spain*

[2]*Departamento de Física Atómica, Molecular y Nuclear, Universidad Complutense de Madrid, Ciudad Universitaria, 28040 Madrid, Spain*

[3]*Department of Chemistry, "Sapienza" University of Rome, P.le A. Moro 5, 00185, Rome, Italy*

[4]*Centre for Medical Radiation Physics, University of Wollongong, Wollongong, NSW 2522, Australia*

(Received 12 June 2012; accepted 10 September 2012; published online 26 September 2012)

We report theoretical integral and differential cross sections for electron scattering from hydrogen cyanide derived from two *ab initio* scattering potential methods. For low energies (0.1–100 eV), we have used the symmetry adapted-single centre expansion method using a multichannel scattering formulation of the problem. For intermediate and high energies (10–10 000 eV), we have applied an optical potential method based on a screening corrected independent atom representation. Since HCN is a strong polar molecule, further dipole-induced excitations have been calculated in the framework of the first Born approximation and employing a transformation to a space-fixed reference frame of the calculated K-matrix elements. Results are compared with experimental data available in the literature and a complete set of recommended integral elastic, inelastic, and total scattering cross sections is provided from 0.1 to 10 000 eV. © *2012 American Institute of Physics*. [http://dx.doi.org/10.1063/1.4754661]

I. INTRODUCTION

It is currently known that the major part of the energy deposited by any kind of primary radiation (x-rays, electrons, positrons, or ions) in biological media is transferred by the secondary electrons produced along the ionization tracks.[1–3] Some medical applications of radiation need accurate interaction models including secondary electron effects. Therefore, in these applications, electron scattering cross sections are required over a wide energy range, from the high energies of the primary particles down to the very low energies of thermalised secondary electrons.

Hydrogen cyanide (HCN) is a linear polyatomic molecule with a high permanent dipole moment of $\mu = 2.98$ D. Numerous biomolecules, including H_2O, have a strong polar nature, which plays an important role in the low-energy scattering dynamics but can cause significant difficulties either for experimental or theoretical studies. Being a fairly simple polyatomic molecule, HCN seems to be an appropriate target for checking computational models of dipole excitations and thus for giving a more realistic comparison between theory and experiments over a very broad range of collision energies which are finally recommended for applicative uses. Given the fact that all previous studies have been limited to a smaller range of collision energies, the present work intends to supply usable data over a much broader region of electron energies.

In the low energy region, electron collisions with HCN have been the subject of numerous studies focused on identifying the low-lying shape resonances and fragmentation paths via dissociative electron attachment (DEA). Early experiments performed by Inoue[4] showed the formation of the anion CN^- via the DEA channel. Burrow *et al.*[5] reported electron transmission spectra and identified a low-lying shape resonance. More recently, May *et al.*[6] reported absolute partial cross sections for the formation of CN^- using a time-of-flight ion spectrometer. Calculations were also performed a while ago by Jain and Norcross[7] using a model potential method and by Varambhia and Tennyson who applied the R-matrix technique.[8] Both studies observed the presence of a low-lying shape resonance around 2.7 eV. In addition, Chorou and Orel[9] calculated the resonance parameters and studied dissociation mechanisms of the molecule using the complex-Kohn variational method in a three-dimensional space.

However, electron scattering studies over wider energy domains are scarce and there is a lack of differential and integral cross section data out of the energy range where resonances take place. To the best of our knowledge, experimental integral and differential elastic cross sections have been only provided by Srivastava and co-workers:[10] they measured elastic differential cross sections for electron impact energies ranging from 3 to 50 eV and scattering angles from 20° to 130° by using a crossed electron-molecular beam technique. Absolute differential cross section values were derived by them through a gas flow procedure for normalisation to helium data. Integral elastic cross sections were also obtained there by extrapolating to angular regions between 0° and 20°

a)E-mail: g.garcia@iff.csic.es.

and from 130° up to 180°. In addition, theoretical elastic cross sections (ECS) and total scattering cross sections (TCS) up to 5000 eV were calculated by Jain and Baluja[11] with a complex optical potential model whose imaginary part is given by a semiempirical absorption potential. Electron impact differential and integral rotational excitation cross sections of HCN can be found in a recent study published by Faure *et al.*[12] where the molecular R-matrix method has been used in combination with the adiabatic-nuclei-rotation approximation.

In this study we report theoretical cross sections for electron scattering from HCN obtained with two different non-empirical quantum scattering models: For low energies a symmetry adapated-single centre expansion approach (ePOLYSCAT) and for higher energies a corrected form of the independent-atom model (IAM) called screening-corrected additivity rule (IAM-SCAR) were used. We have also calculated dipole-induced rotational excitations and then we compared them with the available data. As a result of this study we provide a complete set of recommended integral elastic, inelastic, and total scattering cross sections from 0.1 to 10 000 eV.

In Sec. II of this article we describe the details of our calculation models: ePOLYSCAT and IAM-SCAR. In Sec. III we present and discuss the results of this study. Thereafter, our work is summarized in Sec. IV before drawing some conclusions from this study.

II. THEORETICAL METHODS

A. Symmetry adapted-single centre expansion (SA-SCE) method

The approach we followed to study the low-energy electron interaction with polyatomic molecules is based on a single-centre expansion (SCE) of the target molecule and the incident electron wavefunction around the center of mass of the N + 1 system. Specific details of our procedure have been discussed before;[13,14] therefore, only a brief outline of the method is given in this section.

The collisional process is described in terms of the usual Schrödinger equation within the fixed nuclei approximation, which considers the time scale of the impinging electron motion to be short compared to the molecular vibrations or rotations. Hence, we can separate the electronic contribution from the nuclear motion while the target is held in a frozen geometry during the scattering process:

$$\hat{H}(\boldsymbol{r}, \boldsymbol{X}; \boldsymbol{R})\Psi(\boldsymbol{r}, \boldsymbol{X}; \boldsymbol{R}) = E\Psi(\boldsymbol{r}, \boldsymbol{X}; \boldsymbol{R}), \tag{1}$$

where $\boldsymbol{r}$ represents the scattered electron position, $\boldsymbol{X}$ stands for the target electrons coordinates $\mathbf{x_i}$ (i = 1, …, N), and $\mathbf{R}$ corresponds to the frozen nuclei coordinates $\mathbf{R_\gamma}$ ($\gamma = 1, \ldots, N$) which act as fixed parameters. The electronic scattering Hamiltonian has several contributions,

$$\hat{H}(\boldsymbol{r}, \boldsymbol{X}; \boldsymbol{R}) = \hat{T}_{\text{incident e}^-}(\boldsymbol{r}) + \hat{V}_{\text{interaction}}(\boldsymbol{r}, \boldsymbol{X}; \boldsymbol{R}) + \hat{H}_{\text{target}}(\boldsymbol{X}; \boldsymbol{R}), \tag{2}$$

where $\hat{T}$ is the kinetic energy operator of the incident particle, $\hat{V}$ is the interaction potential between the incoming projectile and the target, and $\hat{H}_{\text{target}}$ is the Hamiltonian of the target molecule.

This is a many electron problem which can be reduced to a set of coupled one-particle equations if the total N + 1 wavefunction is expanded in terms of the target eigenstates,

$$\Psi(\boldsymbol{r}, \boldsymbol{X}; \boldsymbol{R}) = \sum_{\alpha} \mathcal{A}\{F_\alpha(\boldsymbol{r})\psi_\alpha(\boldsymbol{X})\}, \tag{3}$$

$$H_{\text{target}}(\boldsymbol{X})\psi_\alpha(\boldsymbol{X}) = \in_\alpha \psi_\alpha(\boldsymbol{X}), \tag{4}$$

where $\psi_\alpha(\boldsymbol{X})$ are the eigenstates of the target Hamiltonian, $\mathcal{A}$ is the antisymmetrization operator, $F_\alpha(\boldsymbol{r})$ is the continuum electron wavefunction, and $\in_\alpha$ is the electronic eigenvalue for the target state α.

We further approximate the wavefunction at the static-exchange (SE) level with the ground electronic state given by a single Hartree-Fock (HF) determinant in the self-consistent field model. This assumption truncates the expansion in Eq. (3) to only one state ($\alpha = 1$). The post HF correlation and polarization corrections are included by means of model potentials (V^{CP}) added to the SE description.[15] After these approximations, we obtain a set of close-coupling (CC) integro-differential equations:

$$\left[\frac{1}{2}\nabla^2 + (\mathrm{E} - \in)\right] F(\boldsymbol{r}) = \int V(\boldsymbol{r}, \boldsymbol{r}')F(\boldsymbol{r}')d\boldsymbol{r}'. \tag{5}$$

To numerically solve the scattering problem, CC equations are converted into a set of coupled radial equations by applying the previously mentioned SCE method, which implies expanding every function around the centre of mass of the N + 1 system. Therefore, any three-dimensional functions, such as the target molecular orbitals, continuum wavefunction, or the interaction potentials V(**r**), are expanded as a set of symmetry adapted angular functions $X_{hl}^{p\mu}(\theta, \phi)$,

$$F^{p\mu}(\boldsymbol{r}) = \frac{1}{r}\sum_{hl} f_{hl}^{p\mu}(\boldsymbol{r})X_{hl}^{p\mu}(\theta, \phi), \tag{6}$$

where μ is a component of the pth irreducible representation of the point group of the molecule ($C_{\text{inf,v}}$ for HCN) and h indexes all the possible $X_{hl}^{p\mu}$ belonging to a certain irreducible representation ($p\mu$) with the same angular momentum l value.[16] Their radial functions $f_{hl}^{p\mu}(r)$ are represented on a numerical grid.

Once we have expanded all the functions over the symmetry adapted ones, we multiply Eq. (5) by $X_{hl}^{p\mu}(\theta, \phi)$ and integrate over the angular variables which leads to a set of coupled radial equations,

$$\left[\frac{d^2}{dr^2} - \frac{l(l+1)}{r^2} + 2(\mathrm{E} - \in)\right] F_{lh}^{p\mu}(r) = 2\sum_{l'h'} \int V_{lh,l'h'}^{p\mu}(r, r')F_{l'h}^{p\mu}(r')dr', \tag{7}$$

where $V_{lh,l'h'}^{p\mu}(r, r')$ is the potential formed by some diagonal and non-diagonal elements which fully describes the electron-molecule interaction. If we only consider the local electron-molecule interaction, we can reformulate Eq. (7) and get its

homogenous form

$$\left[\frac{d^2}{dr^2} - \frac{l(l+1)}{r^2} + 2(\mathrm{E} - \epsilon)\right] F_{lh}^{p\mu}(r) = 2\sum_{l'h'} V_{lh,l'h'}^{\mathrm{SMECP}}(r) F_{l'h'}^{p\mu}(r), \quad (8)$$

$$\mathrm{V}^{\mathrm{SMECP}}(\mathbf{r}) = \mathrm{V}^{\mathrm{ST}}(\mathbf{r}) + \mathrm{V}^{\mathrm{ME}}(\mathbf{r}) + \mathrm{V}^{\mathrm{CP}}(\mathbf{r}). \quad (9)$$

The potential $\mathrm{V}^{\mathrm{SMECP}}$ refers to the static-model-exchange-correlation-polarization potential. The initial non-local exchange potential has been replaced by a local energy-dependent exchange model potential denoted V^{ME}. The one chosen is the free-electron-gas-exchange potential HFEGE suggested by Hara long ago[17] where the interaction between the bound-electron density, $n(\mathbf{r})$, with the continuum electron, considered as a free electron, gives rise to the exchange term:

$$V_{\mathrm{FEGE}}^{\mathrm{ex}}(\boldsymbol{r}) = -\frac{2}{\pi} k_F(\boldsymbol{r}) \left(\frac{1}{2} + \frac{1-\eta^2}{4\eta} \ln\left|\frac{1+\eta}{1-\eta}\right|\right), \quad (10)$$

where $\eta = k/k_F(\boldsymbol{r})$, k being the single-electron momentum, and $k_F(\boldsymbol{r}) = \{3\pi^2 n(\boldsymbol{r})\}^{1/3}$ is the Fermi momentum of the electron distribution.

The response of the target to the charged projectile is described by the correlation and polarization effects, at short and long range, respectively. This interaction is modelled by an energy-independent local potential V^{CP} which smoothly joins together both contributions at a certain $\mathrm{r}_{\mathrm{match}}$:

$$\mathrm{V}^{\mathrm{CP}} \begin{cases} \mathrm{V}^{\mathrm{corr}}(\mathbf{r}), & \mathbf{r} \le \mathrm{r}_{\mathrm{match}} \\ \mathrm{V}^{\mathrm{pol}}(\mathbf{r}), & \mathbf{r} > \mathrm{r}_{\mathrm{match}} \end{cases}.$$

We have used the Lee-Yang-Parr form for the ($\mathrm{V}^{\mathrm{corr}}$)[18] where an analytical expression of the potential is obtained as a function of the target electronic density. This term is smoothly joined together with the polarization term $\mathrm{V}^{\mathrm{pol}}$ which is a function of the polarization tensor.[18] For a given molecular geometry $\boldsymbol{R}$ it has the following form:

$$V^{pol}(\boldsymbol{r};\boldsymbol{R}) = \lim_{r\to\infty}\left(-\sum_{k=1} \frac{\alpha_k(\boldsymbol{R})}{2r^{2k+2}}\right). \quad (11)$$

With this purely local potential $\mathrm{V}^{\mathrm{SMECP}}$ (**r**) the homogenous radial equation (8) is solved using the standard Green's function technique.[19] In the present case the permanent dipole and quadrupole terms (experimental values) have been added to the long-range part of the static potential, V^{ST} (**r**) defined above using the matching radius of Eq. (11). The asymptotic form of the wavefunction is then analyzed to obtain the scattering K-matrix from which integral and differential elastic cross sections can be computed. This computational method is referred to as "ePOLYSCAT."

However, when the target molecule has a permanent dipole moment as is the case of hydrogen cyanide, the fixed nuclei approximation breaks down and causes divergences in the evaluation of elastic differential cross sections (EDCS) in the forward direction. In order to overcome this drawback another code developed by Gianturco and co-workers has been employed: POLYDCS.[20]

Within this approach the initial, body-fixed K matrices which describe the electron-molecule scattering process, are read and transformed into a space-fixed (SF) frame of reference (laboratory frame). Then SF-K matrices are employed to calculate the state-to-state rotationally elastic and inelastic differential cross section as a Legendre expansion of the solutions. The long-range nature of the dipole potential implies that a very large number of partial waves need to be considered. However a slow convergence of this sum can be avoided by introducing the following formula:

$$\frac{d\sigma}{d\Omega} = \frac{d\sigma^B}{d\Omega} + \sum_{\mathrm{L}} \left(A_L - A_L^B\right) P_L(\cos(\theta)). \quad (12)$$

The first term on the right side represents the analytic Born DCS,[21] while the second term contains the unitarized Born terms (A_L^B) subtracted to the close-coupling calculation (A_L). This formula can be considered as a "correction" of the original Born approximation for polar molecules: short-range effects are introduced by the close-coupling calculation (ePOLYSCAT) summing up terms up to a specific partial wave, while higher partial wave contributions are calculated assuming the Born approximation for an electron-point dipole interaction. Moreover, it has been demonstrated that theoretical DCS does not depend on the initial rotational state;[22] thus, cross sections can be calculated from the rotational ground state of the target ($\mathrm{J} = 0$) to higher rotational states. In these calculations we have included transitions up to $\mathrm{J} = 3$.

B. SCAR method

This second method which permits to study the interaction of intermediate and high energy electrons with molecules is based on a corrected form of the IAM known as SCAR. Details of this method have been presented in previous works,[23–26] therefore, only a brief description is given here.

Initially, this approximation does not consider the molecule as a single target but as an aggregate of atoms which scatter independently assuming that molecular binding does not affect the electronic distribution of the atoms. The first subjects of these calculations are therefore the constituent atoms, namely, H, C, and N. Each atomic target is represented by an interacting complex (optical) potential, $\mathrm{V}_{\mathrm{opt}}(\mathbf{r})$, whose real part accounts for the elastic scattering of the incident electrons while the imaginary part represents the inelastic processes that are considered as "absorption" from the incident beam. This optical potential can be expressed as

$$\mathrm{V}_{\mathrm{opt}}(\mathbf{r}) = \mathrm{V}_{\mathrm{s}}(\mathbf{r}) + \mathrm{V}_{\mathrm{ex}}(\mathbf{r}) + \mathrm{V}_{\mathrm{pol}}(\mathbf{r}) + \mathrm{i}\mathrm{V}_{\mathrm{abs}}(\mathbf{r}), \quad (13)$$

where V_{s} (**r**) is the static term derived from the Hartree-Fock calculation of the atomic charge density.[27] V_{ex} (**r**) is the exchange term which accounts for the indistinguishability between the incident and target electrons. The expression chosen for this term is the semiclassical energy-dependent formula derived by Riley and Truhlar.[28] $\mathrm{V}_{\mathrm{pol}}$ (**r**) is the polarization term which describes the long-range interactions and depends on the target dipole polarizibility in the form given by Zhang *et al.*[29] Finally, the absorption potential $\mathrm{V}_{\mathrm{abs}}$ (**r**), which accounts for the inelastic processes, is based on Staszewska´s quasifree model.[30] Initially, some divergences were found when results were compared to the available atomic scattering data. After including some improvements such as many-body

and relativistic corrections, screening effects inside the atom, local velocity correction, and in the description of the electrons' indistinguishability, the model proves to provide a good approximation for electron-atom scattering[24,25] over a broad energy range. An excellent example of this was for elastic electron–atomic iodine (I) scattering,[31] where the optical potential results compared very favourably with those from a sophisticated Dirac-B-spline R-matrix computation.

Within this model we also numerically integrate the radial scattering equation, from where we obtain the complex partial wave phase shifts δ_l. Using these phase shifts, in combination with the optical theorem, we can generate the atomic scattering amplitudes ($f(\theta)$), which provide differential ($d\sigma_{el}/d\Omega$) and integral (σ_{el}) elastic cross sections as well as the total (σ_{tot}) scattering cross sections as a function of the scattering angle (θ) and the momentum of the incident electrons (k):

$$f(\theta) = \frac{1}{2ik}\sum_{l=0}^{l_{\max}}(2l+1)(e^{2i\delta_l}+1)P_l(\cos\theta),$$

$$\frac{d\sigma_{el}}{d\Omega} = |f(\theta)|^2, \tag{14}$$

$$\sigma_{el} = \int \frac{d\sigma_{el}}{d\Omega}d\Omega, \quad \sigma_{tot} = \frac{4\pi}{k^2}Imf(\theta=0). \tag{15}$$

In order to obtain molecular cross sections, the IAM has been followed by applying a coherent addition procedure, commonly known as the additivity rule (AR). In this approach, the molecular scattering amplitude ($F(\theta)$) is derived from the sum of the above atomic amplitudes which lead to the differential elastic cross section for the molecule ($d\sigma^{\text{molec}}/d\Omega$), according to

$$F(\theta) = \sum_{\text{atoms}} f_i(\theta)e^{i\mathbf{q}\mathbf{r}_i},$$

$$\frac{d\sigma_{el}^{\text{molecule}}}{d\Omega} = \sum_{i,j} f_i(\theta)\, f_j^*(\theta)\frac{\sin qr_{ij}}{qr_{ij}}, \tag{16}$$

where $\mathbf{q}$ is the momentum transferred in the scattering process and r_{ij} is the distance between the i and j atoms.

Integral elastic cross sections for the molecule can be determined by integrating Eq. (16). Alternatively, elastic cross sections can be derived from the atomic scattering amplitudes in conjunction with the optical theorem[24] giving

$$\sigma_{el}^{\text{molecule}} = \sum_{\text{atoms}} \sigma_{el}^{\text{atom}}. \tag{17}$$

Unfortunately, in its original form, we found an inherent contradiction between the integral cross section derived from those two approaches, which suggested that the optical theorem was being violated.[32]

The main limitation of the AR is that no molecular structure is considered, thus it is really only applicable when the incident electrons are fast enough to effectively "see" the target molecule as a sum of the individual atoms (typically above ~100 eV). To reduce this limitation we developed the SCAR method[25,26] which considers the geometry of the corresponding molecule (atomic positions and bond lengths) by introducing some screening coefficients which modify both differential and integral cross sections, especially for decreasing energies.[25,26] With this correction the range of validity of the IAM-SCAR method might be extended down to about 30 eV. For intermediate and high energies (30–5000 eV) this method has been proved to be a powerful tool to calculate electron scattering cross sections from a high variety of molecules of very different sizes, from diatomic to complex biomolecules.[33]

From the above description of the IAM-SCAR procedure it is obvious that vibrational and rotational excitations are not considered in this calculation. However, for polar molecules such as HCN additional dipole-induced excitation cross sections can be calculated following the procedure suggested by Jain.[34] Basically it calculates differential and integral rotational excitation cross sections for a free electric dipole in the framework of the first Born approximation (FBA) which can be incorporated to our IAM-SCAR calculation in an incoherent way, just adding the results as an independent channel. Although rotational excitation energies are, in general, very low (typically a few meV) in comparison with the incident electron energies, in order to validate the Born approximation the latter energies should be higher than about 20 eV. Under these circumstances, rotational excitation cross sections J → J′ were calculated by weighting the population for the Jth rotational quantum number at 300 K and estimating the average excitation energy from the corresponding rotational constants. We can call the whole procedure as the IAM-SCAR + rotations method and it has been successfully used for other polar molecules as H_2O and pyrimidine.[35,36]

Additionally, when the permanent dipole moment of the molecule is at least as large as is the case of HCN, the FBA also fails for medium and large scattering angles. In order to partially solve this situation, we introduced a correction based on that suggested by Dickinson,[37] which brings a substantial improvement for electron scattering cross sections with strongly polar molecules. This procedure introduces a first-order corrective term to the differential cross sections ($\frac{d\sigma^{Dck}}{d\Omega}$) for medium and large angles but maintaining the FBA correction ($\frac{d\sigma^{B}}{d\Omega}$) for lower angles:

$$\frac{d\sigma^{B}}{d\Omega} \approx \frac{D^2}{6E_i}\frac{1}{\sin^2(\theta/2)} \quad \theta < \theta_c, \tag{18}$$

$$\frac{d\sigma^{Dck}}{d\Omega} \approx \frac{\pi D}{64E_i}\frac{1}{\sin^3(\theta/2)} \quad \theta > \theta_c, \tag{19}$$

where D is the permanent dipole moment of the molecule and E_i is the energy of the projectile. Providing that the dipole moment is bigger than $D = 0.75$ Dy, both curves smoothly join together at θ_c, the critical angle at which they cross each other.

III. RESULTS AND DISCUSSION

A. Integral elastic cross sections

For low energies, integral ECS have been computed with the ePOLYSCAT model. The initial target wavefunction was generated by the GAUSSIAN 94 code[38] at the Hartree-Fock level and expanded in the 6-311++G (3df,3pd) basis set. The

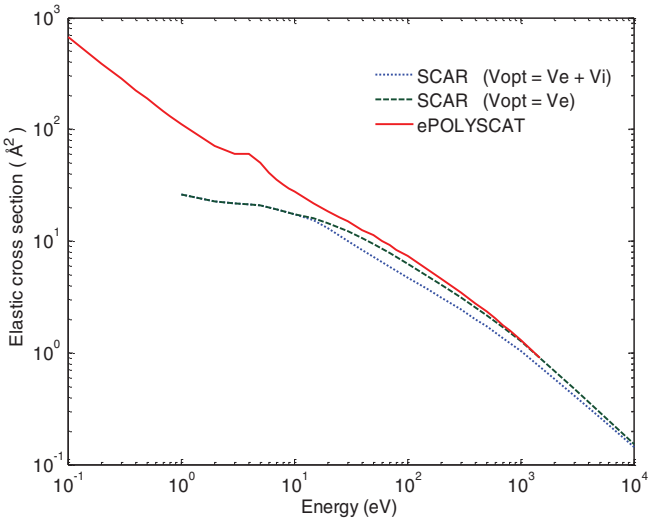

FIG. 1. Integral elastic cross sections. ePOLYSCAT (solid red line), SCAR (dotted blue line), SCAR without the absorption potential term (dashed green line).

bound and scattering orbitals were expanded at the center-of-mass of the target including partial waves up to $l_{max} = 60$. The multipolar expansion of the potential V^{SMECP} included terms up to $\lambda_{max} = 120$. The scattering at short-range was carried out up to $R_{max} = 11.5$ Å and the discrete (r,θ,φ) grid of the scattered wavefunction involved a total of 1464 × 84 × 324 points. The computed dipole moment from our ground state wavefunction turned to be 3.26 D, while the experimental value is 2.98 D:[39] the latter was the one used for the long-range part of the static interaction. This modification is expected to affect final cross sections mainly at very low collision energies, while the other contributions of the model potential terms are more important at energies away from threshold.

For higher incident electron energies, ECS for HCN have been computed with the IAM-SCAR model. The corresponding atomic cross sections for C, N, and H were previously calculated and discussed.[25] Molecular cross sections have been calculated according to available geometrical parameters:[40] $r_{CN} = 1.136$ Å and $r_{CH} = 1.05$ Å.

Results for both calculations are plotted in Fig. 1. We expect the ePOLYSCAT cross sections to be more reliable for energies below the ionisation threshold (13.6 eV), while the more favourable energies to apply the IAM-SCAR procedure are above 30 eV. Based on previous studies using both methods,[35,41,42] we can establish a numerical uncertainty of up to about 10% for the integral cross sections provided by each method in its own energy range of applicability. As seen from Fig. 1, within 15 and 30 eV, ePOLYSCAT (solid red line) and SCAR (dotted blue line) elastic cross sections differ from one to another by 50%. This discrepancy may be due to the optical potential V_{opt} used by ePOLYSCAT which, although allowing for virtual excitations to be included globally during the scattering process, does not allow for direct electronic excitations to take part in the collisional event. We have shown, however, that scattering calculations ignoring inelastic processes overestimate integrated elastic cross sections for energies above the ionization limit.[23] In fact, when the absorption term is removed from the SCAR optical potential (dashed green line), calculated ECS values increase and both methods tend to converge to the same values for increasing energies. So that, we propose in this range (15 to 30 eV) ECS data derived from a smooth interpolation between both data curves by means of a double logarithmic fitting with an estimated error of about 20%. The ePOLYSCAT data have used its K-matrix values to obtain Born-corrected cross sections via the procedure described for the POLYDCS code.

B. Rotational excitations

Rotational excitations are very important for molecules with strong permanent dipole moment, such as HCN, and especially for low electron energies. However, the excitation energy associated to rotational levels is so low and the angular distribution of scattered electrons is so peaked in the forward direction that experiments do not have enough energy and angular resolution to distinguish these inelastic processes from the elastic one. Thus, for a more realistic comparison between theoretical and experimental ECS, additional rotational excitations have been calculated with both methods.

Computational results have been compared with the experimental data from Srivastava *et al.*[10] available in the literature. They measured elastic differential cross sections from 20° to 130° for electron impact energies of 3, 5, 11.6, 21.6, and 50 eV. In order to obtain integral ECS they extrapolated to small angles (0°–20°) following the Born approximation, and to higher angles by simply extending the straight line defined by the last measured points. Authors stated that due to insufficient electron energy resolution of the experimental device, their elastic term includes also rotational and vibrational excitations.

Cross sections calculated with POLYDCS (solid red line) and IAM-SCAR + rotations method (dashed blue line) together with the experimental data (green dots) are shown in Fig. 2. At intermediate energies, 11.6 eV and 21.6 eV, both calculations agree with Srivastava's measurements, within the error limits. However, at lower energies (3 and 5 eV)

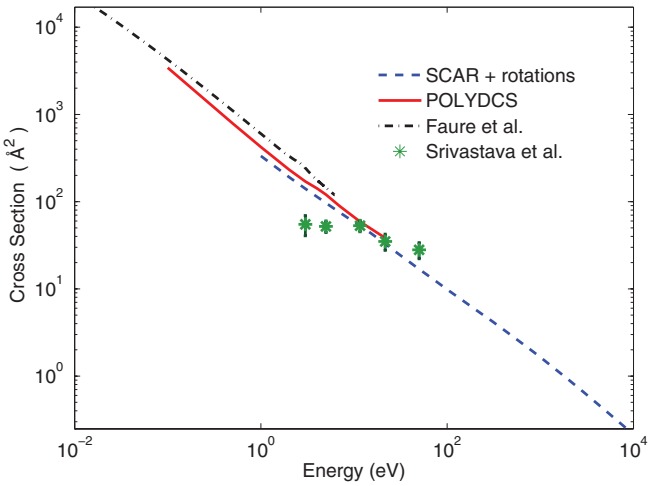

FIG. 2. Elastic cross sections plus rotational excitation cross sections. POLYDCS (solid red line), SCAR (dashed blue line), Faure *et al.*[12] (dotted-dashed black line), Srivastava *et al.*[10] experimental data (∗).

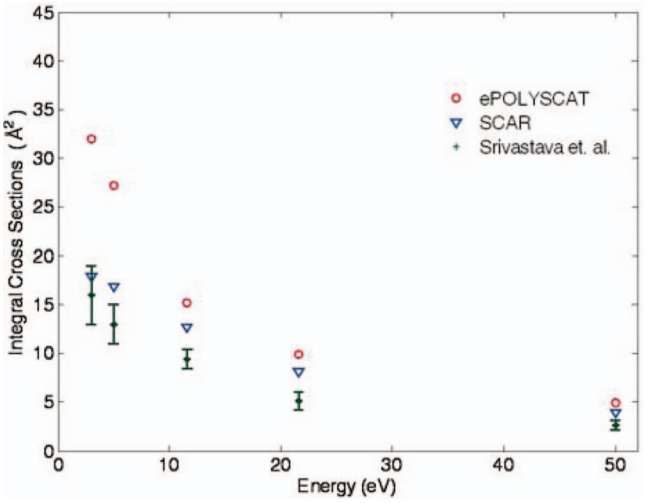

FIG. 3. Elastic cross sections integrated from 20° to 130°. ePOLYSCAT (O), SCAR (∇), Srivastava *et al.*[10] experimental data (∗).

experimental ECS are lower than the calculated values. This may be due to the extrapolation method used[10] in the experiments for low angles ($\theta < 20^\circ$) following the first Born approximation. It has been proved by Mittleman and von Holdt[43] that the FBA underestimates the cross sections for polar molecules and they claim that in the case of HCN molecules it could lower the results by a factor of 2 at low energies. Note, in fact, that below 5 eV reasonable agreement between the present calculation and that by Faure et *al.*[12] has been found (see Fig. 2). This suggests us to integrate experimental and theoretical data only from 20° to 130° (see Fig. 3), avoiding any approximation. As may be seen in this figure, now the agreement is much better, especially with the SCAR calculation, verifying that discrepancies in the integral ECS (0°–180°) results are due to errors in the extrapolation procedures used by Srivastava *et al.*[10]

As a result of this discussion we propose the set of recommended integral cross section data which is shown in Table I. As mentioned above, low energy data are provided by the ePOLYSCAT-POLYDCS calculations while above 30 eV, the SCAR data have been preferably considered, both with an estimated error of about 10%. The smooth interpolation method applied between 30 and 50 eV leads to an uncertainty between 10 and 20% for the recommended values in this energy range.

C. Total cross sections

As far as we know, there are no experimental data of TCS for HCN. Hence, our results are compared in Fig. 4 with the theoretical ones provided by Jain and Baluja,[11] who calculated TCS for electron scattering energies from 10 to 5000 eV. These authors used a complex optical potential composed of static, exchange, polarisation, and absorption terms. The imaginary part of this potential, absorption term, was based on that given by Staszewska[30] but substituting the threshold excitation energy Δ of the original formulation by the ionization potential, which they claimed to be closer to the "mean excitation energy" of the target. Within this approach, rotational excitations were included by taking into

TABLE I. Recommended electron elastic, rotational, electronically inelastic (electronic excitation and ionization), and total scattering cross sections for HCN molecules from 0.1 to 10 000 eV.

Energy (eV)	Elastic (Å²)	Rotational (Å²)	Electronically Inelastic (Å²)	Total (Å²)
0.1	668.95	2765.47		3434.43
0.2	389.05	1416.22		1805.27
0.3	282.14	1005.86		1288.00
0.4	224.79	749.21		974.00
0.5	188.44	597.56		786.00
0.6	163.59	503.61		667.20
0.7	145.31	431.49		576.80
0.8	131.25	378.35		509.60
0.9	120.24	339.96		460.20
1	111.60	311.84		423.44
2	70.73	163.76		234.50
3	60.86	109.41		170.26
4	60.42	81.50		141.92
5	50.50	70.20		120.71
7	35.48	53.62	3.94	93.04
10	26.72	39.75	5.70	72.17
11.6	23.75	34.76	6.42	64.94
15	19.36	27.75	6.96	54.07
20	15.41	21.57	7.08	44.06
21.6	14.40	20.25	7.06	41.71
30	11.05	15.22	6.74	33.01
40	8.80	11.82	6.28	26.90
50	7.54	9.54	5.86	22.95
70	6.00	6.87	5.19	18.06
100	4.73	5.10	4.70	14.53
150	3.72	3.53	4.06	11.31
200	3.11	2.72	3.61	9.44
300	2.42	1.88	2.93	7.22
400	2.00	1.43	2.48	5.91
500	1.72	1.15	2.16	5.04
700	1.36	0.85	1.71	3.92
1000	1.04	0.61	1.32	2.97
2000	0.59	0.32	0.76	1.68
3000	0.42	0.22	0.54	1.18
5000	0.27	0.14	0.35	0.75
10 000	0.14	0.07	0.19	0.40

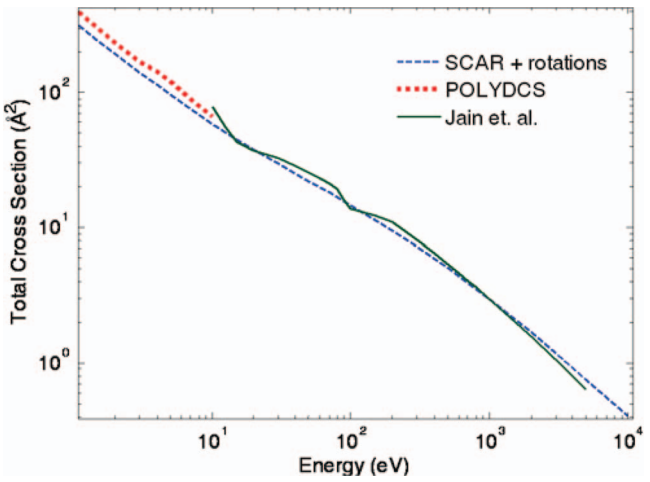

FIG. 4. Total cross sections. POLYDCS (dotted red line), SCAR (dashed blue line), and Jain and Baluja[11] (solid green line).

account the anisotropic terms in the multipole expansion of the optical potential within the FBA.

Jain's TCS results are quantitatively similar to the SCAR data; however, at high energies Jain's values tend to decay faster but discrepancies remain within the estimated error limits for the whole energy range where the comparison is feasible. One should note, however, that the calculations of Ref. 11 employed a simpler description of both target state and interaction potentials, so that they refer to a lower level of numerical accuracy with respect to the present study.

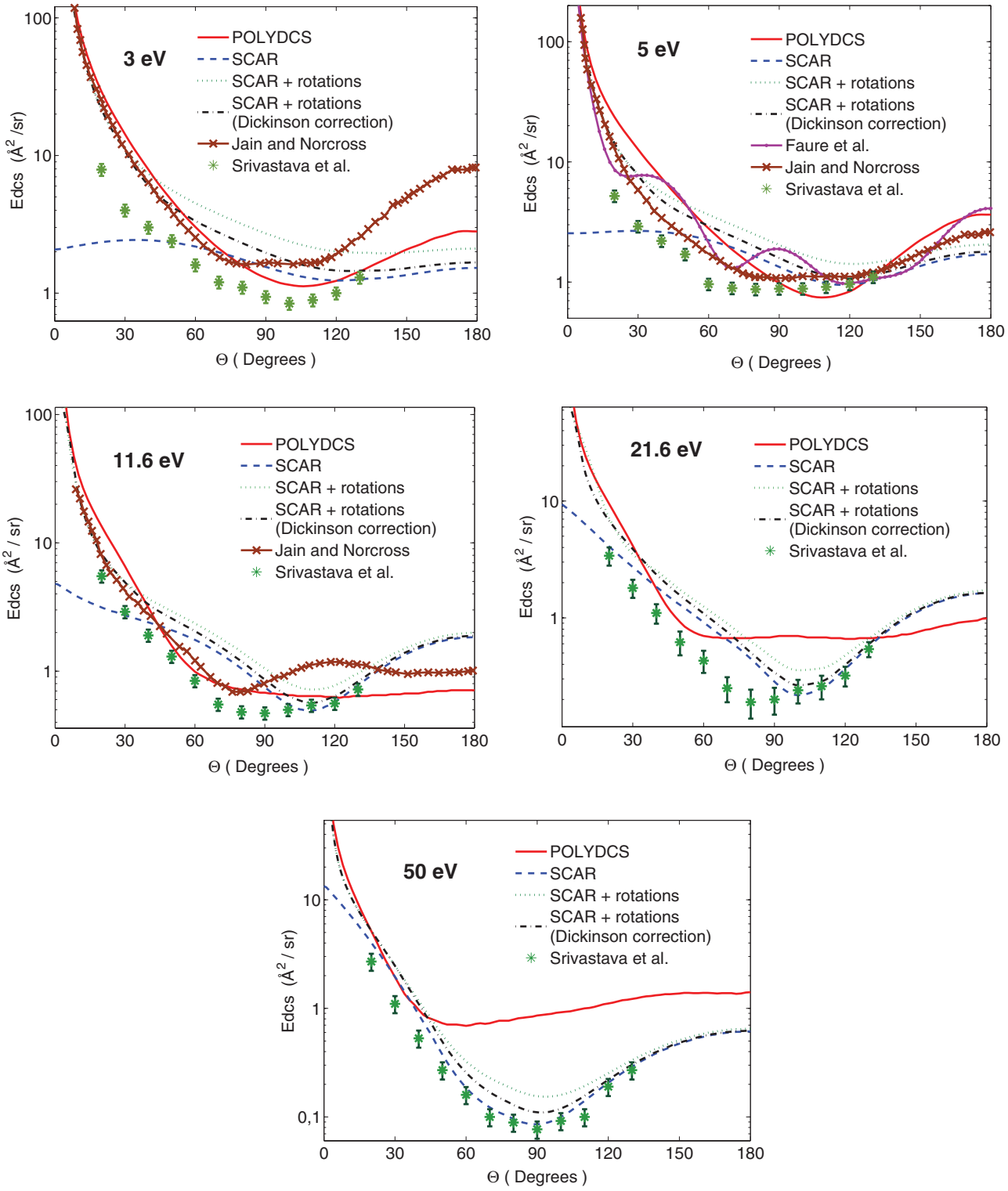

FIG. 5. Elastic differential cross sections: SCAR (dashed blue line). EDCS + rotation excitations: POLYDCS (solid red line), SCAR + rotations (dotted green line), SCAR + rotations with Dickinson correction (dashed-dotted black line), Jain and Norcross[7] model potential (solid-crossed brown line), Faure *et al.*[12] R-matrix method calculation (solid-dotted purple line), Srivastava *et al.*[10] experimental data (green asterisk).

Below the first electronic excitation energy, i.e., below 6.15 eV,[44] elastic collisions constitute the main scattering process. Up to that energy, recommended TCS values are given by the POLYDCS computational model, including rotational excitation cross sections. Above 30 eV recommended TCS data come from the IAM-SCAR + rotations model which accounts for electronic and rotational excitations as well as ionisation processes. Again, a double logarithm interpolation procedure has been carried out to derive data within both limits.

D. Differential elastic cross sections

Calculated EDCS have been compared with experimental data for energies of 3, 5, 11.6, 21.6, and 50 eV (see Fig. 5). As we mentioned in Sec. III B, experimental EDCS could not resolve rotational excitations. Therefore, to allow the comparison, we have also plotted in Fig. 5 calculated differential cross sections including rotational excitations (POLYDCS and SCAR + rotations)

At low energies (3, 5, and 11.6 eV), POLYDCS qualitatively agrees with the experimental results verifying its reliability at energies below 15 eV. The ePOLYSCAT calculations without the FBA correction, not shown in Fig. 5, exhibit diffuse undulating structures at the lower scattering energies due to the breakdown of the body-fixed approximation for polar molecules, as we have already discussed in Sec. II A. The effect from a space-fixed treatment is included in the calculations with the POLYDCS programme. For these energies, there is a reasonable agreement between this calculation and those from Jain and Norcross[7] and Faure *et al.*[12]

At higher energies, EDCS values from the IAM-SCAR method show good agreement with the experimental data. For instance, at E = 21.6 eV, for small and large angles ($\theta = 20^\circ$, 30°, 90°, 100°, 110°, 120°, and 130°), calculated values are within the experimental error bars being the difference less than 10%. The situation gets even better at E = 50 eV, where for $\theta > 50^\circ$ IAM-SCAR data are in excellent agreement with measurements and for $\theta > 80^\circ$ divergences are less than 10%. As expected, for this relatively high energy and for the relatively large scattering angles attainable by Srivastava's apparatus, their measurements, and our SCAR calculations, without including rotations, agree very well.

However, when rotational excitations based on the FBA (IAM-SCAR + rotations) are considered, differential cross sections tend to overestimate the experimental data at medium and large angles for increasing energies. This effect is even more remarkable for the POLYDCS calculation which also includes rotational excitations. It is known that the FBA approximation fails for relatively large scattering angles when the permanent dipole moment of the target is remarkable, as is the case of HCN. As shown in Fig. 5, this situation is partially solved by applying the Dickinson's correction[31] which mainly affects large angles.

IV. CONCLUSIONS

In this article we have reported calculated electron collisional data with the hydrogen cyanide molecule. Two different methods have been employed to provide elastic cross sections: the ePOLYSCAT, which is known to be reliable for energies below 15 eV, and the IAM-SCAR which gives accurate results for E > 30 eV. Both methods were consistent within their respective energy range of applicability, where the estimated errors are lower than 10%. This situation allowed a simple interpolation between 15 and 30 eV, providing data for this range with associated uncertainties between 10% and 20%.

Since HCN has a strong permanent dipole moment, additional dipole-induced rotational excitation cross sections have been further included, within the framework of the first Born approximation, to realistically compare our differential cross section data with those measured by Srivastava *et al.*[10] Under these conditions we have found a reasonable agreement for all the energies where direct measurements are available and especially at 50 eV where the SCAR data lie within the experimental error limits. Due to the angular limitation of the experiment (20°–130°), integral values provided by Srivastava and co-workers included some approximations to extrapolate data to low and high angles. The low angle region becomes particularly sensitive to dipole-induced rotations at low energies and cross sections could vary significantly depending on the approximation applied. Therefore, we have compared integrated elastic cross sections from 20° to 130°, finding an excellent agreement within 10% for energies ranging from 3 eV to 50 eV.

In addition, a complete set of integral cross sectional data including elastic, rotational excitation, electronically inelastic (electronic excitations and ionization), and total cross sections has been provided from 0.1 to 10 000 eV. As mentioned above, data derived from each quantum scattering model are recommended in their respective energy range of effectiveness, while a double logarithmic fitting is applied to smoothly join them together at intermediate energies.

We can finally conclude that a combination of the described theoretical approaches allows obtaining reliable electron scattering data over a very broad energy range even for strong polar molecules. This result becomes really promising to study more complex biological targets, as the DNA and RNA constituents, which are being demanded by important biomedical applications of radiation both for diagnostics and therapy.

ACKNOWLEDGMENTS

This work is partially supported by the Spanish Ministerio de Economía y Competitividad (Project No. FIS2009-10245) and the EU/ESF COST Action MP1002 "Nanoscale Insights into Ion Beam Cancer Therapy (Nano-IBCT)." M.C.F. is granted by the Comunidad Autónoma de Madrid local government. One of us (F.A.G.) also thank the Italian MUIR for support through the PRIN 2009-2012 projects.

[1] C. von Sonntag, *The Chemical Basis of Radiation Biology* (Taylor and Francis, London, 1987).
[2] B. Boudaiffa, P. Cloutier, D. Hunting, M. A. Huels, and L. Sanche, Science **287**, 1658 (2000).

[3]B. D. Michael and P. O'Neill, Science **287**, 1603 (2000).
[4]M. Inoue, J. Chim. Phys. Phys.-Chim. Biol. **63**, 1061 (1966).
[5]P. D. Burrow, A. E. Howard, A. R. Johnston, and K. D. Jordan, J. Phys. Chem. **96**, 7570 (1992).
[6]O. May, D. Kubala, and M. Allan, Phys. Rev. A **82**, 010701 (2010).
[7]A. Jain and D. W. Norcross, Phys. Rev. A **32**, 134 (1985).
[8]H. N. Varambhia and J. Tennyson, J. Phys. B **40**, 1211 (2007).
[9]S. T. Chourou and A. E. Orel, Phys. Rev. A **80**, 032709 (2009).
[10]S. K. Srivastava, H. Tanaka, and A. Chutjian, J. Chem. Phys. **69**, 1493 (1978).
[11]A. Jain and K. L. Baluja, Phys. Rev. A **45**, 202 (1992).
[12]A. Faure, H. N. Varambhia, T. Stoecklin, and J. Tennyson, Mon. Not. R. Astron. Soc. **382**, 840 (2007).
[13]I. Baccarelli, F. A. Gianturco, A. Grandi, and N. Sanna, Int. J. Quantum Chem. **108**, 1878 (2008).
[14]F. A. Gianturco and R. R. Lucchese, J. Phys. Chem. A **108**, 7056 (2004).
[15]F. A. Gianturco, A. Jain, and L. C. Pantano, J. Phys. B **20**, 571 (1987).
[16]F. A. Gianturco, D. G. Thompson, and A. Jain, *Computational Methods for Electron-Molecule Collisions* (Plenum, New York, 1995).
[17]S. J. Hara, J. Phys. Soc. Jpn. **22**, 710 (1967).
[18]C. Lee, W. Wang, and R. G. Parr, Phys. Rev. B **37**, 785 (1998).
[19]R. R. Lucchese and F. A. Gianturco, Int. Rev. Phys. Chem. **15**, 429 (1996).
[20]N. Sanna and F. A. Gianturco, Comput. Phys. Commun. **114**, 142 (1998).
[21]L. A. Collins and D. W. Norcross, Phys. Rev. A **18**, 467 (1978).
[22]Y. Okamoto, K. Onda, and Y. Itikawa, J. Phys. B **26**, 745 (1993).
[23]F. Blanco and G. Garcia, Phys. Lett. A **295**, 178 (2002).
[24]F. Blanco and G. García, Phys. Rev. A **67**, 022701 (2003).
[25]F. Blanco and G. Garcia, Phys. Lett. A **317**, 458 (2003).
[26]F. Blanco and G. Garcia, Phys. Lett. A **330**, 230 (2004).
[27]R. D. Cowan, *The Theory of Atomic Structure and Spectra* (University of California Press, London, 1981).
[28]M. E. Riley and D. G. Truhlar, J. Chem. Phys. **63**, 2182 (1975).
[29]X. Z. Zhang, J. F. Sun, and Y. F. Liu, J. Phys. B **25**, 1893 (1992).
[30]G. Staszewska, D. W. Schwenke, D. Thirumalai, and D. G. Truhlar, Phys. Rev. A **28**, 2740 (1983).
[31]O. Zatsarinny, K. Bartschat, G. Garcia, F. Blanco, L. R. Hargreaves, D. B. Jones, R. Murrie, J. R. Brunton, M. J. Brunger, M. Hoshino, and S. J. Buckman, Phys. Rev. A **83**, 042702 (2011).
[32]J. B. Maljković, A. R. Milosavljević, F. Blanco, D. Šević, G. García, and B. P. Marinković, Phys. Rev. A **79**, 052706 (2009).
[33]F. Blanco and G. García, Phys. Lett. A **360**, 707 (2007).
[34]A. Jain, J. Phys. B **21**, 905 (1988).
[35]A. Muñoz, J. C. Oller, F. Blanco, J. D. Gorfinkiel, P. Limão-Vieira, and G. García, Phys. Rev. A **76**, 052707 (2007).
[36]A. Zecca, L. Chiari, G. García, F. Blanco, E. Trainotti, and M. J. Brunger, J. Phys. B **43**, 215204 (2010).
[37]A. S. Dickinson, J. Phys. B **10**, 967 (1977).
[38]M. J. Frisch, G. W. Trucks, H. B. Schlegel *et al.*, GAUSSIAN 03, Revision C.02, Gaussian, Inc., Wallingford, CT, 2004.
[39]R. L. DeLeon and J. S. Muenter, J. Chem. Phys. **80**, 3992 (1984).
[40]See the chemical information database at http://chem.sis.nlm.nih.gov/chemidplus/.
[41]F. A. Gianturco and R. R. Lucchese, J. Chem. Phys. **108**, 6144 (1998); **114**, 3429 (2001).
[42]M. C. Fuss, A. Muñoz, J. C. Oller, F. Blanco, M. J. Hubin-Franskin, D. Almeida, P. Limao-Vieira, and G. García, Chem. Phys. Lett. **486**, 110 (2010).
[43]M. H. Mittleman and R. E. von Holdt, Phys. Rev. **140**, A726 (1965).
[44]A. K. Nayak, R. K. Chaudhuri, and S. N. L. G. Krishnamachari, J. Chem. Phys. **122**, 184323 (2005).